

New trends and future perspectives on plasma focus research

Leopoldo Soto

Comisión Chilena de Energía Nuclear, Casilla 188-D, Santiago, Chile

E-mail: lsoto@cchen.cl

Received 29 October 2004

Published 20 April 2005

Online at stacks.iop.org/PPCF/47/A361

Abstract

This paper includes a brief overview of the contributions and results of several groups working in plasma focus (PF) devices around the world in the last few years. In section 2 a summary of the most important results of the dense transient plasma research programme of the Comisión Chilena de Energía Nuclear is presented. An approach to an integrated vision of the present PF research status is presented in the next section. Some parameters that remain practically constant in PF devices that operate in a wide range of energies from 1 MJ to tens of joules are discussed. These parameters ('plasma energy density parameter' and 'drive parameter') are used as a design tool to achieve an ultra-miniature pinch focus device operating at energies less than 1 J. Preliminary results of such an ultra-miniature device are presented. Applications to non-destructive tests, detection of substances, pulsed radiation in biology and material sciences are also briefly discussed in this paper.

1. Introduction and general overview

A plasma focus (PF) is a kind of pinch discharge. It reproduces the scenario of high energy density, intense beams of charged and neutral particles and radiation emission. Thus it becomes a laboratory for fundamental and applied research related to fusion, neutron production, hard x-ray and high brightness soft x-ray production and astrophysical phenomena. There are some reviews about PF research and applications: an extensive review can be found in [1]. This paper does not pretend to be a whole review. It is only intended to give the author's vision of the new trends and future perspectives of PF research.

This paper is divided into five sections. Section 1 is an introduction and brief overview including contributions and results of several groups around the world in the last few years. The presentation of the results has been divided according to the physical topics rather than to the kind or size of machine. The following topics are discussed: a brief phenomenological description, a presentation of the experimental facilities related to PF research, a summary

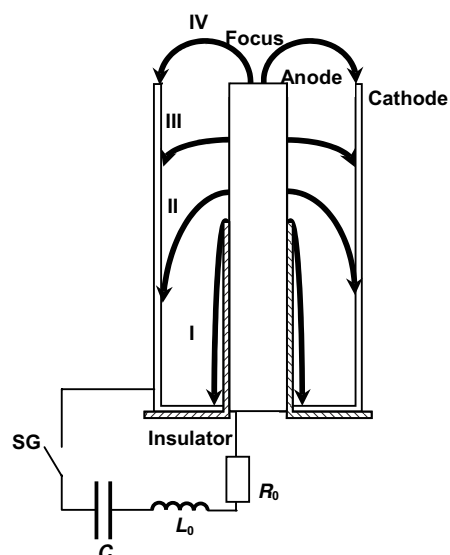


Figure 1. A schematic of the circuit and the plasma dynamics is shown. The capacitor C is discharged over the electrode through a spark gap (SG). The plasma dynamics is sketched in a side section of the electrodes. I, discharge starts over the insulator; II, III, the current sheath is accelerated along the coaxial electrodes; IV, pinch.

about theoretical models for PF description and recent advances related to the characteristics and mechanisms of emission of neutrons, x-rays and ions. The phenomenological description is illustrated with results obtained in the Comisión Chilena de Energía Nuclear (CCHEN). Section 2 is a summary of the most important results of the dense transient plasma research programme of the CCHEN. Examples of applications are shown in each of the above sections where applicable. In section 3, I intend to present an integrated vision of the present PF status discussing the meaning and use of parameters that remain practically constant in PF devices that operate in a wide range of energies, from 1 MJ to tens of joules. The ‘plasma energy density parameter’ and the ‘drive parameter’ are discussed. The possibility of enhancing the thermonuclear component of the neutron yield by increasing the drive parameter (or the velocity of the plasma sheath) is also analysed. Thus, in section 4 the plasma energy density parameter and the drive parameter are used like design tools to achieve an ultra-miniature pinch focus device operating with energy less than 1 J. Preliminary results of such an ultra-miniature device are presented. In section 5, final comments are presented.

A PF is a kind of pinch discharge in which a high-pulsed voltage is applied to a low-pressure gas between coaxial cylindrical electrodes, generating a short-duration, high-density plasma region in the axis. Two geometries were proposed for these devices, differing in their electrode aspect ratio (electrode length divided by inner electrode diameter): the Filipov configuration [2], with an aspect ratio < 1 (typical values are 0.2), and the Mather configuration [3], with an aspect ratio > 1 (typically 5–10).

Figure 1 shows a scheme of the equivalent electrical circuit and the discharge evolution in a Mather type PF. The electrodes are in the vertical position: the anode in the centre is partially covered from its base by a coaxial insulator. The discharge starts over the insulator surface and then the plasma sheath comes off and is accelerated axially by the magnetic field auto-generated by the current. After the current sheath runs over the upper end of the central

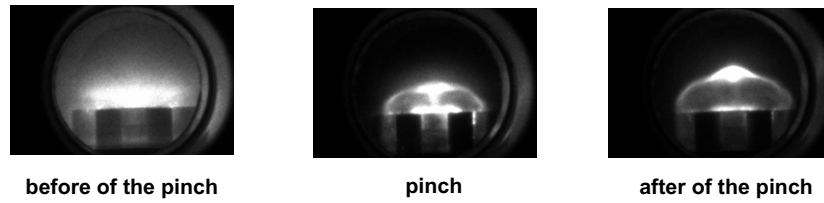


Figure 2. The typical sequence of the plasma dynamics in PF discharges (these correspond to discharges in hydrogen at 0.47 mbar in a PF of only 50 J and were obtained with a ICCD camera gated at 5 ns exposure time [30]).

electrode, the plasma is compressed in a small region (the focus or pinch). In the majority of devices these three stages last a few microseconds, and less than 500 ns in a new generation of fast plasma foci. The maximum pinch compression should coincide with the peak current in order to achieve the best efficiency. Depending on the energy of the pulse power generator, the current in the pinch varies from tens of kiloamperes to some mega-amperes. The velocity of the current sheath is of the order of $1 \times 10^5 \text{ m s}^{-1}$ in the axial phase and of the order of $2.5 \times 10^5 \text{ m s}^{-1}$ in the pinch compression. The pinch generates beams of ions and electrons, and ultra-short x-ray pulses. The duration of these pulses is of the order of tens to hundreds of nanoseconds. In the pinch the temperature is of the order of 200 eV–1 keV and the density is $\sim 10^{24} - 10^{26} \text{ m}^{-3}$. Using deuterium gas, PF devices produce fusion D–D reactions, generating fast-neutron pulses ($\sim 2.5 \text{ MeV}$) and protons (leaving behind ^3He and ^3H). Figure 2 shows photographs from visible light of the plasma that illustrate the dynamics of a PF.

From the electrical point of view a good approximation of the equivalent electrical circuit for the pulse power system is a capacitor of capacity C_0 , an equivalent series inductance L_0 (it includes the inductances of the capacitor, transmission line and connections and switches) and an equivalent series resistance, R_0 , of the circuit. The plasma is considered as an inductance and resistance with temporal dependence $L_p(t)$ and $R_p(t)$. Figure 1 shows the equivalent circuit.

The equations describing the dependence of current and voltage in the circuit are:

$$V_0 - \frac{1}{C_0} \int I dt - \frac{d}{dt}(L_0 I) + R_0 I = V_p(t),$$

$$V_p = \frac{d}{dt}(L_p I) + R_p(t) I.$$

The inductance associated with the plasma column in the radial phase can be written as:

$$L_p = \frac{\mu_0}{2\pi} z_p \ln \frac{b}{r_p},$$

where z_p and r_p are the length and the radius of the plasma column and b is the radius of the cathode.

The resistance associated with the plasma column in the radial phase can be written as:

$$R_p = \frac{z_p}{\sigma \pi r_p^2}.$$

The electrical conductivity, σ , would have an anomalous term.

Figure 3(a) shows typical waveforms for the time derivative of the current and voltage. A large change in the plasma impedance in the final stage of the radial compression (principally in the inductance) produces the ‘dip’ observed in the dI/dt signal and the peak observed in the

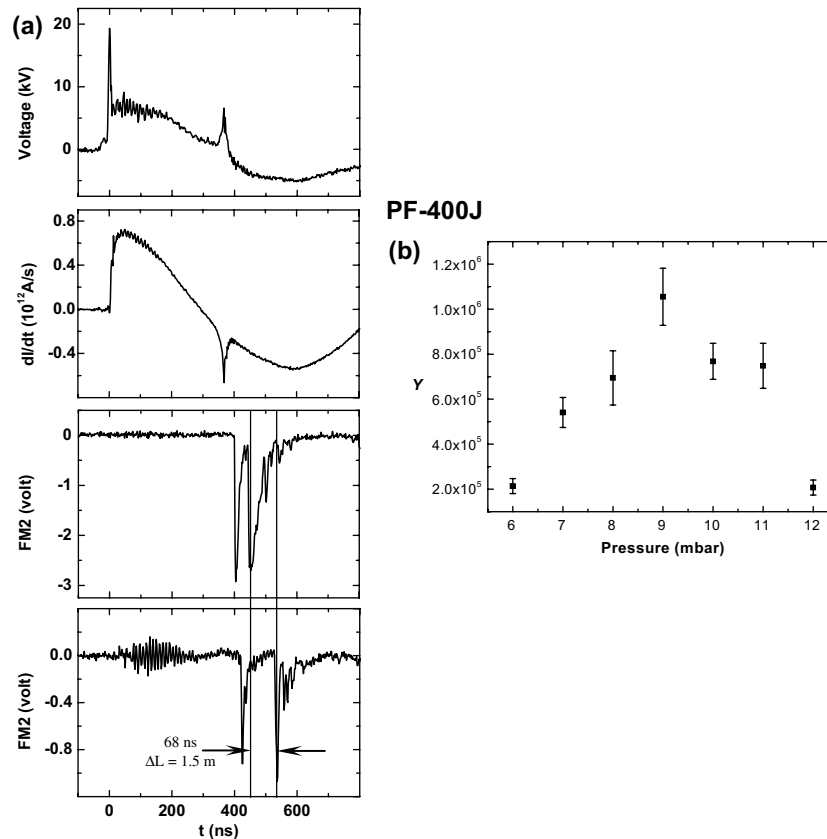


Figure 3. (a) Typical electrical signals of a PF discharge. The signals correspond to a discharge in deuterium at some millibars pressure in a device of 400 J [32] at the CCHEN. Signals with a scintillator with a photomultiplier (FM1 and FM2) are also shown. The distance ΔL , between FM1 and FM2, was $\Delta L = 1.5$ m, and the time of flight for the neutrons was ~ 68 ns; thus the energy of the neutrons was ~ 2.77 MeV. (b) Neutron yield against the filling gas pressure for the PF-400J.

voltage signal. These features in the electrical signals are considered evidence of pinch or focus in the plasma column. The maximum pinch compression should be nearly coincident with the peak current in order to achieve the best efficiency. Signals obtained with two detectors based on a plastic scintillator–photomultiplier combination located at two different distances from the plasma show two moments of radiation signals. First, a x-ray signal appears and then a neutron signal is observed. From the time of flight analysis, the energy of the neutrons is measured and a value of the order of 2.5 MeV is determined. It is important to note that these signals could have a more complex temporal structure; in fact in big PF experiments the neutron signal has two or three pulses. Figure 3(b) shows the dependence of the total neutron yield, Y , with the deuterium filling pressure, p , of the discharge showing high and low deuterium pressure limits for the neutron production.

In spite of the supersonic radial velocity, for a simple description in the final stage of the radial compression it is plausible to assume that the plasma column can be described by the Bennett equilibrium. In fact, if the radial velocity of the pinch boundary is much less than the Alfvén speed, the evolution of the pinch phase is quasi-static, and the well-known Bennett relation obtained from the equilibrium between the thermal pressure and the magnetic pressure acting upon the plasma is applicable. Assuming a homogeneous temperature profile

and the same temperature, T , for ions and electrons, Bennett found a fundamental relation $16\pi NkT = \mu_0 I^2$, where k is the Boltzmann constant and N is the number of charged particles per unit length, i.e. the electron density, n , integrated across the plasma column section. It is important to note that the Bennett relation stands independent of the shape of the ion density, n , and current density, J . Thus, the Bennett relation essentially gives the average temperature for a given line density N and for a given total current I through the plasma column.

In spite of all the accumulated research related to plasma foci, several questions remain unanswered, particularly those concerning the sheath formation, insulator conditioning, influence of gas impurities and radiation emission mechanisms involved in the transient plasma processes occurring during the pinch.

An area of research that has not been well explored is that of very-low-energy PF devices. The energy stored in the pulsed power generator of the device in order to drive the PF ranges from large devices of 1000 kJ to small devices of a few kilojoules. Most of the experimental studies were focused on medium and large facilities that use a pulsed power generator charged from tens to hundreds of kilojoules, or small devices of only a few kilojoules. In fact, we can question whether good focusing can be achieved using a device with a generator with less than 1 kJ, and if so which are the appropriate design criteria and scaling laws in this energy region. On the other hand, there is a permanent and growing interest in the research community to understand how the x-rays, neutrons and charged particles are produced in pinches. How they are produced is still an open question, at least in the sense of allowing for the design of optimized devices for applications. Recently, the PF has attracted the attention of the plasma research community because of its use in pulsed radiation applications. It is important to remark that the PF is a pulsed non-radioactive source. The emitted neutrons could be applied to perform radiographs and substance analysis, taking advantage of the penetration and activation properties of neutral radiation. The intense x-ray pulses produced by bremsstrahlung radiation from localized electron beams and from hot-spots are excellent candidates for radiography of moving or wet objects and for microelectronic lithography [21–23].

1.1. PF devices in a wide range of energies

1.1.1. Conventional devices. PF devices have been constructed in a variety of sizes in correlation with the energy stored in the pulsed electrical generator, ranging from kilojoules [4, 5] to megajoules [6], producing neutron pulses from 10^7 to 10^{12} neutrons per shot. In the last decade more laboratories have been equipped with Mather type PF, and a few laboratories are still working with Filippov type PF (e.g. DENA device [7]). Some of the devices used in the last decade are: PF-1000, a MJ device in Poland [6, 8, 9]; PF-360, a device of 360 kJ, also used in Poland [10]; SPEED2, a device in the range 70–100 kJ in Germany until the year 2001 [11], currently at CCHEN in Chile [12]; and several devices in the range of 2–7 kJ, NG1 [13] and PACO [14] in Argentina, PF at PUC in Chile [15], Fuego Nuevo II in Mexico [16], DPF-2.2 in China [17], a 5.5 kJ PF device in Iran [62], a 7 kJ PF device in Japan [63], 4 kJ PF device at IC in England [18], PFIPS in Korea [83], UNU/ICTP-PFF, a device designed and constructed by the Asian–African Association for Plasma Training Network (AAAPT) and in operation in several countries [4, 5, 19, 20]. Specifically in the range of around 3 kJ there are numerous results obtained by the AAAPT.

1.1.2. Repetitive devices. Repetitive PF devices for x-ray production have been reported by Lebert *et al* [24] and Prasad *et al* [25], both with 2–5 kJ of electrical energy stored in the capacitor bank and a repetition rate of the order of 2 Hz and by Lee *et al* [26] with 3 kJ and

1.9 kJ, and a 3 Hz and 16 Hz repetition rate, respectively. A PF of 6 kJ and a 1 Hz repetition rate for neutron production has also been reported [27].

1.1.3. SPEED devices. SPEED devices are generators based on Marx technology and were designed in the University of Düsseldorf. These kinds of devices drive a fast PF where the maximum current is achieved in 400 ns or less. The special design produces a device with an impedance of the order of the pinch impedance (of the order of 100 mΩ), making it more efficient in the transference of energy to the plasma. The SPEED2 [11] consists of 40+/- Marx modules connected in parallel. Each module has six capacitors (50 kV, 0.625 μF, 20 nH) and three spark gaps (SGs), and so the pulse power generator SPEED2 is a medium-energy and large-current device (SPEED2: 4.1 μF equivalent Marx generator capacity, 300 kV, 4 MA in short circuit, 187 kJ, 400 ns rise time, $dI/dt \sim 10^{13} \text{ A s}^{-1}$) [2]. The SPEED2 is currently in Chile at the CCHEN. It arrived in May 2001 from Düsseldorf University, Germany, and it has been in operation since January 2002, becoming the most powerful and highest-energy device for dense transient plasmas in the Southern Hemisphere. Simultaneously, an intermediate device, SPEED4, was constructed. It consists of 4+/- Marx modules connected in parallel. Each module has two capacitors and one SG (50 kV, 0.625 μF, 20 nH). This device is currently being set up (SPEED4: 1.25 μF equivalent Marx generator capacity, 100 kV, 550 kA, 350 ns rise time, $dI/dt \sim 10^{12} \text{ A s}^{-1}$).

1.1.4. Compact devices with energy lower than 1 kJ. An area of research that is not well explored is that of very-small, low-energy plasma foci. Feasibility objections have been made to devices with lower energies (less than 1 kJ), for not having enough energy and time to create, move and compress the plasma. In the first stage of a programme to design a repetitive pulse radiation generator for industrial applications, at the CCHEN, we constructed two very small plasma foci operating at an energy level of the order of (a) hundreds of joules (PF-400J, 880 nF, 20–35 kV, 176–539 J, ~300 ns time to peak current) [31] and (b) tens of joules (PF-50J, 160 nF capacitor bank, 20–35 kV, 32–100 J, ~150 ns time to peak current) [28–30]. These very small devices produce pinch plasmas, neutrons and x-rays pulses, thus showing that the objections were not applicable [28–33].

1.2. Models and simulations

A useful goal to have is a theoretical or numerical model that allows the design of a specific PF, predicting the plasma dynamics, the temperature and the subsequent emission of particles and radiation.

The main dynamical properties of the PF discharge evolution, such as acceleration and implosion times, can be computed reasonably well in the zero-dimensional approximation by a snowplough equation. However, it is well known that this model, when it is applied to a radial compression, gives a zero-radius column. Lee [4, 35] developed a model using a snowplough model for the axial phase and a slug model (with structure) for the radial phase. This model shows that the axial velocity and the radial velocity of the current sheath are proportional to $(I_0/ap^{1/2})$, where I_0 is the peak current intensity, a is the anode radius and p is the gas filling pressure for the maximum neutron yield. $(I_0/ap^{1/2})$ is called the ‘drive parameter’. A similar parameter has been discussed earlier [36]. Further results of this model show that the pinch length, z_p , and the pinch radius, r_p , are proportional to the anode radius, $z_p = 0.8a$ and $r_p = 0.12a$ [37].

Recently, the PLADEMA Network led by Clause and Moreno has developed three models of PF operation. These three models are based on the MHD theory with the snowplough

approximation. In a simple conceptual model [34] the zero-dimensional MHD equations are solved for the run-down stage to calculate the focus current in a Mather type PF. In the radial phase, the plasma column is simulated as a cylindrical oscillator linearized about the Bennett equilibrium. This idealization yields analytical expressions for the neutron yield and the focus time as functions of the design parameters (geometrical magnitudes of the electrodes, external capacity and inductance) and operational conditions (pressure, initial voltage). The quantitative calculations require experimental calibration of two shape parameters, accounting for the fact that the actual current sheath is not planar, and one effective thermodynamic coefficient represents the entropic state of the pinch. A second model, a lumped parameter model of PF [42], follows the Lee model of coupled axial and radial planar pistons [4, 34]. This lumped model was validated against a large set of experimental data covering a wide range of energies from some kilojoules to near 1 MJ. The user needs to provide five effective parameters: axial and radial shape coefficients, axial and radial piston densities in terms of the stagnant density, and a radial velocity profile parameter. Finally, a finite-element model of the PF dynamics has been developed by the PLADEMA Network [43]. The current sheath is represented by a set of axisymmetric segments acting as articulated magnetic pistons. In this way the shape evolution of the current sheath coupled with the electric circuit can be tracked throughout all the stages of the discharge (for different arrays and shapes of electrodes and insulators) without the introduction of any effective parameter.

More complex models such as two-dimensional MHD simulations have been used by several authors to calculate the dynamics of PF discharges. These models were developed 30–40 years ago (see, e.g. [76]). To obtain a good quantitative agreement with experimental results, computer codes which are based on more sophisticated physical models are necessary. The main phase of the current sheath in the PF evolution should be described in the frame of a non-ideal MHD model. However, it can be supplemented by taking into account atomic processes (i.e. ionization) in a neutral gas. Recently the MHD equations of such a code were applied to the conditions of the big machine PF-1000 in Poland (100 kJ, 2 MA, 12 cm anode radius, 4 mbar deuterium filling pressure) [9]. The maximum current obtained from the computations is about 15% greater than the measured value. The velocity computed for the run-down phase is also greater ($\sim 20\%$) than the measured value. The current sheath shape obtained from the simulation agrees qualitatively with the experimental results obtained with fast framing cameras [9]. The computer simulations were stopped at the instant of the current sheath stagnation near the pinch axis, when the MHD model is not valid anymore. When the shock wave reaches the pinch axis, an ion temperature of the order of 1.2 keV and a plasma density of the order of $5 \times 10^{25} \text{ m}^{-3}$ in the plasma column are obtained from the computations. There are not enough experimental data for this phase to compare with the computations.

On the other hand, Milanese and Pouzo [38, 39] have studied the reasons for the existence of high and low deuterium pressure limits beyond which the neutron yield drops even when the pinch current is, respectively, increasing or monotonically decreasing. With respect to the upper pressure limit, it was found that an insufficiency in the energy available for ionizing the gas swept during the roll-off stage produces an inefficient pinch compression and a drop in the neutron yield. The lower pressure limit was explained in terms of the presence of a radiative wave produced by an excess of plasma energy during the radial compression stage. Also, they have proposed a possible explanation for the empirical scaling law for neutron yield with the pinch current in terms of both thermal and non-thermal nuclear fusion processes [40]. Based on the results obtained in these first two stages, the authors created criteria for designing the PF device and improving its performance for nuclear fusion production [41].

1.3. Neutrons

Using deuterium gas, PF devices produce fusion D–D reactions, generating fast-neutron pulses (~ 2.5 MeV, tens to hundreds of nanoseconds of duration) and protons (leaving behind ^3He and ^3H).

The mechanisms of nuclear fusion and the subsequent neutron production in pinch discharges are still an open and controversial field. The participation of two main processes in the production of the total neutron yield, Y , by a pinch discharge is widely accepted: thermonuclear fusion and ion beam–target fusion. Thus, the total neutron yield is $Y = Y_{\text{th}} + Y_{\text{b-t}}$, where Y_{th} is the thermonuclear component and $Y_{\text{b-t}}$ is the beam–target component. If the fusion mechanism is thermonuclear, an isotropic emission is expected. Experimentally, more emission is observed in the axial direction (0°) than in the radial direction (90°). Usually, these measurements are made simultaneously with two detectors, and the ratio between those is considered a characterization of the anisotropy, Y_0/Y_{90} being of the order of 1.4–3 in most of the PF devices. This measurement anisotropy is attributed to a non-thermal process of the ion beam–target between the deuterons with the plasma and with the neutral gas. In addition, time of flight measurements of the neutron energy result in a distribution of energy with a maximum energy greater than 2.45 MeV (which is the energy of thermonuclear neutrons). This could indicate that additional energy from an energetic beam is transferred in the fusion reaction to the emitted neutrons.

Scaling laws for the neutron yield with the peak current have been proposed. Theoretically, it is possible to show the thermonuclear fusion scale with the peak current as $Y_{\text{th}} \propto I_0^4$. For the beam–target fusion two scaling laws have been proposed. In [40], assuming that the ion beam current is proportional to the pinch current, the relation $Y_{\text{b-t}} \propto I_0$ is obtained, while in [44], from an inductive model for the beam acceleration, the relation $Y_{\text{b-t}} \propto I_0^{4.5}$ is obtained.

Using the results of several devices in a wide range of energies and currents (1 kJ to 1 MJ and 100 kA to 1 MA), the most accepted empirical scaling law for the total neutron yield, Y , is $Y \propto I_0^{3.3}$ [35]; however, other dependences also based on experimental results have been proposed, for example, $Y \propto I_0^{4.7}$ [14, 40].

In [45] Moo *et al* reported an investigation of the ion beam of a PF of 3.3 kJ using a metal obstacle and a deuterated obstacle. The neutron emission is measured with time-integrated detectors. It is found that in the normal operation of the focus without a target obstacle, less than 15% of the neutrons are produced within the pinch column, and more than 85% of the neutrons arise from the deuterium ion-beam bombardment of the deuterium gas in a region that is over the plasma pinch region.

Measurements of neutron emission with more angular resolution have been developed [46, 47]. A study using time-resolved detectors (plastic scintillator in combination with photomultiplier) in the axial (0°), radial (90°) and 45° directions is presented in [46]. The presence of two periods of neutron emission was found in a medium-energy (28 kJ) PF. The first period occurs when the tight plasma column is being formed before the disruption of the plasma column and lasts some tens of nanoseconds. The second period is longer, three to four times longer. The overall emission shows anisotropy (with respect to the pulse length) between the end-on (0°) and side-on directions (90°).

In experiments carried out in the PF-360 facility operated without and with a planar solid target of D_2O , temporal changes in the anisotropy of the neutron were observed [77]. The neutron signals (in the axial and in the radial directions) appear to be composed of three sequential pulses. Even though time-integrated measurements show an anisotropy of $Y_0/Y_{90} \sim 1.8$ in both cases, with and without a D_2O target, the temporal pulses show a time dependent anisotropy. In contrast to the one which we would expect for the beam–target

mechanism, with the D₂O target the anisotropy coefficient of the third pulse was noticeably lower than that observed without the target (1.03 compared with 1.81).

In [47] Castillo *et al* reported time-integrated measurements of the neutron emission from -90° to 90° including nine angles of view. The neutron flux was measured with CR-39 nuclear track detectors covered with polyethylene. The angular measurements were compared with the total neutron yield (the angular integral of the measurements). The results are consistent with an angular uniform plateau (isotropic emission) plus a shape peaked in the direction of the axis of the discharge (anisotropic emission). Using this analysis the authors obtain an interesting result. Seventy per cent of the total neutron emission is isotropic and only 30% is anisotropic because the axial emission is concentrated only in a small solid angle, being its contribution to the total emission, lower in comparison with the isotropic emission. The value usually reported as the ratio between the axial and radial measurements may be misleading.

Composite loads in PF have been experimentally studied in big devices in order to increase the neutron yield from PF discharges. For example, needle and planar D₂O-ice targets, as well as D₂ gas puffs, have been used in Poland [59, 61]. On the other hand, the influence of preionization around the insulator sleeve of the PF by a mesh type β -source $^{28}\text{Ni}^{63}$ on neutron emission has been investigated by Zakaullah *et al* [56] in a small device. The neutron emission has been found to increase up to 25%. The results of this experiment suggest that preionization may be helpful in designing a device as a sealed neutron source for different field applications.

1.4. X-rays

In the last decade the studies related to the x-ray emission from PF devices have been devoted to (a) characterization of the soft x-rays from the plasma column and hot-spots in discharges operating with gases with atomic number higher than hydrogen (neon, argon, xenon, etc) [5] and mixtures of gases [15], characterization of the hard x-rays from the interactions of energetic electron beams impacting on the anode; (b) the PF as an x-ray source for applications (x-ray ‘nanoflash’); and (c) x-ray studies using composite loads in PF devices as gas puffed PF [57] and wire in PF discharges [58].

An exhaustive study on x-ray characteristics from a PF of ~ 3 kJ (UNU/ICTP-PFF device, AAAPT) has been conducted by the group of Zakaullah. In [48] it is estimated that about 40 J of energy is radiated as x-rays, out of which 8 J is in the form of Cu-K $_{\alpha}$ lines in 4π geometry. The radiation yield represents a system efficiency of 1.7% for overall x-ray emission and 0.35% for the Cu-K $_{\alpha}$ line [49]. It is also found that with the same scaling law with the current peak, the Cu-K $_{\alpha}$ emission varies as $Y_K [\text{J}] \sim [E(\text{kJ})]^{3.5-4.5} \sim [I(100 \text{ kA})]^{3.5-4.5}$, whereas the total x-ray emission is found to follow $Y_{\text{tot}} [\text{J}] \sim [E(\text{kJ})]^{4.5-5.5} \sim [I(100 \text{ kA})]^{4.5-5.5}$. The emission is dominated by the interaction of electrons in the current sheath with the anode tip. With a cut at the anode tip, the x-ray flux in the side-on direction is increased three times.

Recently, studies of x-ray polarization from hot-spots have been conducted by Jakubowski *et al* [78, 79]. Measurements of spectral lines using two spectrographs with perpendicular dispersion planes were performed. The most important results of the spectral measurements appear to be an evident difference between the relative intensities of the same lines, registered with the two perpendicular spectrographs. Such a difference could be explained by the x-ray polarization, caused possibly by the interaction of fast electron beams.

From the point of view of applications, the feasibility of a small PF as a high-intensity flash x-ray source for good contrast biological radiography has been demonstrated in several laboratories (see, e.g. [14, 49]).

For industrial uses a significant contribution is being developed by the PLADEMA network led by Clause and Moreno. Tomography using ultra-fast radiographies obtained with a PF has been developed [50, 51]. The radiographies are obtained with hard x-rays outside the stainless steel discharge chamber in a PF device of 4.7 kJ. The effective energy of these x-rays is estimated at ~ 120 keV. The spatial resolution of the final tomography is greater than that obtained in a single x-ray radiography. Currently, these techniques are being successfully applied in quality assurance programmes for the automotive industry [52].

1.5. Ions

Depending on the power supply energy levels, the ion energy of the beam is of the order of 100–1000 keV. The acceleration mechanisms that produce such ion beams are not yet completely understood. Extensive studies of ion beams have been performed in order to learn about acceleration mechanisms in the last 40 years, and recently to study non-linear processes in dense magnetized plasmas. Detailed measurements of an ion mass- and energy-spectrum as well as an ion angular distribution have been carried out in Poland in the last few years (see, e.g. [6, 80]). In [80] the correlation between the appearance of hot-spots and the emission of intense x-rays, relativistic electron beams and ion beams has been studied. The experiments were performed in the PF device MAJA (44 kJ, 35 kV, 500 kA maximum current). Measurements in the axial direction have shown that PF discharges emit collimated pulsed ion beams from hot-spots inside the dense plasma column. The energy spectrum of the accelerated deuterons extends up to 1 MeV, and its maximum appears in the range 400–450 keV.

Other research work in a small PF device of 3 kJ has been conducted by groups of the AAAPT to study the energy spectrum of the axially emitted deuteron beam [81]. In these experiments the deuteron energy ranges from 80 to 250 keV, with a more frequent energy range between 90 and 140 keV.

From a theoretical point of view, an approach to studying the deuteron motion in a filamentary PF for different configurations of filaments has been developed by Pasternak and Sadowski [84]. Their results show that the current filaments can cause peculiarities in the angular distribution of deuterons emitted from a PF pinch column.

In addition, in the last few years, the study and characterization of the ion beams emitted from a PF has also been motivated by its use in material science. Ion implantation, energetic ion irradiation, surface modification and coating production are some of the uses of the ion beams and hot plasma streams from PF devices [19, 53–55, 85]. Applications of fast ions for the production of isotopes useful in nuclear medicine have also been suggested [82].

1.6. Plasma temperature greater than 100 keV?

Results that indicate electron and ion temperatures greater than 100 keV from hot-spots in a PF are claimed by Lerner [74]. On the other hand, such ion temperatures have recently been measured in pinches from wire arrays using the Z-accelerator at Sandia [75]. An explanation of the observations obtained in Sandia has been proposed by Haines in terms of the ion viscous heating due to MHD instabilities in a Z-pinch [75]. If the results claimed by Lerner are correct, it would mean a rebirth of the PF as a fusion energy device. This should be investigated in other PF devices by means of complementary diagnostics of the temperature, like spectroscopy, Doppler broadening and x-ray images from the plasma. Lerner also proposes the use of the PF for $p^{11}\text{B}$ fusion.

Table 1. The principal parameters of the PF devices at the CCHEN are listed.

Device	PF-50J	PF-400J	SPEED4	SPEED2
Capacity (μF)	0.160	0.880	1.25 ^a	4.16 ^a
Charging voltage (kV)				
Maximum	35	35	100	300
Typical operation	25–30	30	60	180
Inductance (nH)	38	38	40	20
Time to peak current (ns)	150	300	350	400
Stored energy (kJ)				
Maximum	0.1	0.54	6.25	187
Typical operation	0.05–0.07	0.4	2.25	67
Peak current (kA)				
Maximum	70	168	550	4000
Typical operation	50–60	127	330	2400
Anode radius (cm)	0.3	0.6	1.6	5.4
Cathode radius (cm)	1.1	1.3	4.5	11
Effective anode length (cm)	0.48	0.7	1–2	1.5–2.5
Insulator length (cm)	2.4	2.1	2.7–3.9	6.5

^a Equivalent capacity of the SPEED generators.

2. Dense transient plasma research programme at CCHEN

At present the Plasma Physics and Plasma Technology Group of the CCHEN has the experimental facilities for studying dense transient discharges, particularly plasma foci in a wide range of energies (50 J to 100 kJ) and currents (40 kA to MA) of the same time scale. In table 1 the principal parameters of the PF devices at the CCHEN are listed.

The programme research includes: (a) the mechanism of x-ray emission (thermal versus beam bremsstrahlung), the mechanism of neutron emission (thermonuclear versus beam-target) and charged particles beam emission; (b) the development of diagnostics; (c) the development of optimized and compact apparatus for flash sources of neutrons and x-rays (nanoflashes) and its possible applications; and (d) studies about how to enhance the drive parameter (related to the plasma sheath velocity) and its role in the thermonuclear component of the neutron yield. This last topic has been recently included. Special efforts have been made towards the miniaturization of PF devices.

Several diagnostics have been implemented: voltage, total current and current derivative monitors; plasma images with an intensified CCD camera gated at 4 ns exposure time; silver activation counter and ³He detectors for neutron yield measurements; a plastic scintillator with a photomultiplier for x-ray and neutron detection with temporal resolution; VUV and soft x-ray spectroscopy; and pulsed optical refractive diagnostics using a pulsed Nd–YAG laser.

2.1. Results in compact devices PF-50J and PF-400J

Compact and fast plasma foci devices were designed and constructed by CCHEN, PF-400J and PF-50J (for details see [31,32]). The size of these devices is of the order of 25 cm \times 25 cm \times 50 cm. The design calculations indicate that neutron yields of 10^4 – 10^5 neutrons per shot are expected with discharges when deuterium is used in the PF-50J and 5×10^5 – 5×10^6 neutrons per shot in the PF-400J. A special technique was developed to detect neutron pulses of the order of 10^4 neutrons per shot. A conventional neutron detection technique using ³He proportional counters was adapted for measuring low neutron yields from D–D fusion pulses [69].

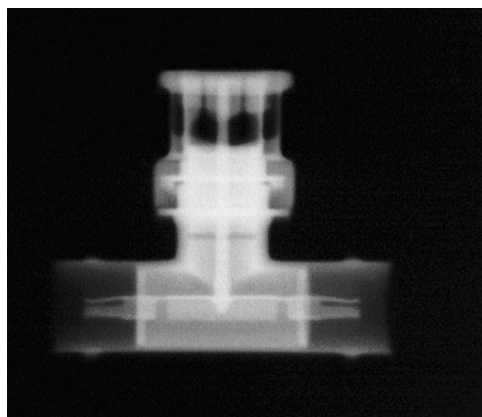


Figure 4. Radiography of a stainless steel BNC 'T' connector obtained with multiples shots using the PF-400J at CCHEN; the internal structure made of metal is easily identified [73].

Neutron emission studies were performed in discharges in deuterium at different pressures, 5–12 mbar, at a charging voltage of 30 ± 2 kV in the PF-400J and 29 ± 2 kV– 25 ± 2 kV in the PF-50J (~ 400 J and ~ 70 – 50 J stored in the capacitor bank, respectively). The typical dip in the signals of the current derivative associated with the formation of a pinched plasma column on the axis was observed in both devices [31, 32]. From the current derivative signals the implosion time (pinch time, measured at the moment of the minimum in dI/dt) versus filling pressure was obtained. The maximum compression of the plasma occurs close to the peak current for a pressure around 7 mbar in the PF-400J and close to 6 mbar in the PF-50J. Signals from two detectors based on a plastic scintillator connected to a photomultiplier were also obtained. Energy of the order of (2.42 ± 0.39) MeV and (2.29 ± 1.28) MeV has been estimated for the PF-400J and PF-50J from time of flight measurements.

The neutron yield as a function of the filling gas pressure was obtained. The maximum measured neutron yield was $(1.06 \pm 0.13) \times 10^6$ neutrons per shot at 9 mbar in the PF-400J [31] and $(3 \pm 1.5) \times 10^4$ neutrons per shot at 9 mbar in the PF-50J operating at 70 J and $(1.1 \pm 0.5) \times 10^4$ neutrons per shot at 6 mbar in the PF-50J operating at 50 J [33]. Figure 2 corresponds to images from the PF-50J. Figure 4 corresponds to the results of the PF-400J device.

Although the measured neutron yield is low in comparison with devices operating at a few kilojoules, this kind of very small device could be operated easily in a repetitive regime from some hertz to kilohertz, increasing the radiation flow, offering space for useful applications.

Potential applications of small and repetitive PF devices are substance detection by transient activation analysis, x-ray imaging and neutrography. In figure 4 a radiography of a stainless steel BNC 'T' connector obtained after multiple shots using the PF-400J is shown; the internal structure made of metal is easily identified [73].

On the other hand, based on commercial information readily available from the internet on fast neutron radiography using a CCD coupled to a Gd converter, it may be concluded that with the proposed 10^6 neutrons per shot source and placing the sample 5 cm from the source, a 5 cm^2 analysis area may be recorded with 10^3 – 10^4 shots, depending on the sample nature and shape. With a 10 Hz repetition rate, this flow will be attained after 100–1000 s. The device presented here, conceived for laboratory purposes, is a single shot machine, which can be operated only at 0.25 Hz. According to the same commercial information, sources providing 10^6 – 10^8 neutrons s^{-1} at a 10 kHz repetition rate are useful for prompt gamma neutron analysis. This translates to 10^2 – 10^4 neutrons per shot.

Table 2. Summary of the results related to the neutron yield obtained in the experiments presented in this paper. The neutron yield measured in Düsseldorf for SPEED2 is also shown [68].

Device	PF-50J	PF-400J	SPEED4	SPEED2	
Operation energy (kJ)	0.05	0.07	0.4	1.56	67
Operation pressure (mbar)	6	9	9	2–9	2–3
Peak current (kA)	50	60	127	280	2400
Neutron yield (neutrons)	(1.1 ± 0.5) × 10 ⁴	(3.3 ± 1.6) × 10 ⁴	(1.06 ± 0.13) × 10 ⁶	—	~10 ¹¹ –10 ¹² (Düsseldorf) [68] ~2 × 10 ¹⁰ (CCHEN)

2.2. Preliminary results in SPEED2 and SPEED4

Most of the previous experiments conducted in SPEED2 at Düsseldorf were done in a PF configuration for x-ray emission, and the neutron emission from SPEED2 was not completely studied. The Chilean operation has begun implementing and developing diagnostics in a conventional PF configuration in order to characterize the neutron emission. Then, after getting the experimental expertise with SPEED2, new experiments in a quasi-static Z-pinch [64–67], gas puffed PF and wires array will be performed to extend the device capabilities. Also, SPEED2 and SPEED4 will be used in the development of applications for radiation pulses from hot, dense plasmas, including x-ray and neutron radiography, detection of substances and micro-radiography for applications to microelectronic lithography and diagnostics of nanostructures. The PF on SPEED2 is an intense pulsed source of neutrons (10^{11} – 10^{12} neutrons per pulse) and x-rays. PF in SPEED4 with heavy gases will be used as an intense source of soft x-rays. The applications will be developed using the above generators in order to determine the radiation threshold for the various types of applications (radiography, neutrography, substance detection). This information will be used to design smaller devices suited for these applications. The Chilean operation of the SPEED2 device has begun implementing and developing diagnostics in a conventional PF configuration. Discharges in PF mode have been performed in Chile at ± 30 kV charging voltage (i.e. 180 kV, 67 kJ). A peak current greater than 2 MA was achieved.

SPEED2 uses a special insulator, quartz covered with alumina, and it requires several shots of preparation in order to obtain a neutron yield with dispersion lower than 30% between shots. We have not had enough shots with the same insulator in order to achieve the proper conditions of operation. Preliminary results obtained at CCHEN show a neutron yield of the order of 10^{10} neutrons per shot: the maximum value obtained up until now at CCHEN is 2×10^{10} neutrons per shot. In Düsseldorf a neutron yield of the order of 10^{11} – 10^{12} neutrons per shot was obtained [68]. Time resolution neutron detection is now being implemented.

SPEED4 has been assembled; however, evidence of pinch in the electrical signals has not yet been observed.

In summary, as part of the research programme at CCHEN, two very small plasma foci have been designed, constructed and set in operation, one of them in the range of hundreds of joules (PF-400J) and the other one in the range of tens of joules (PF-50J). The region of tens of joules was unexplored until now. The neutron emission against filling pressure has been obtained in both devices [31, 33]. A special technique was developed to detect neutron pulses of the order of 10^4 neutrons per shot [69]. The maximum measured neutron yield was of the order of 10^6 and 10^4 neutrons per shot in the PF-400J and PF-50J, respectively. On the other hand, preliminary results on neutron emission from SPEED2 have been obtained. In table 2 the results related to the neutron yield obtained in the experiments at CCHEN are shown.

Table 3. The density energy parameter, $28E/a^3$, and the drive parameter ($I_0/ap^{1/2}$) are listed for various PF devices: E is the stored energy in the capacitor bank, I_0 is the peak current, a is the anode radius and p is the gas filling pressure for the maximum neutron yield. The energy density parameter has a value of the order of $(1-10) \times 10^{10} \text{ J m}^{-3}$ for all the machines listed. The drive parameter has practically the same value for all the machines listed ($68-95 \text{ kA cm}^{-1} \text{ mbar}^{1/2}$) with the exception of SPEED2.

Device [reference]-location	Energy E (kJ)	Anode radius a (cm)	Peak current (kA)	Pressure (mbar)	Energy density parameter $28E/a^3$ (J m^{-3})	Driven factor $I_0/ap^{1/2}$ ($\text{kA mbar}^{-1/2} \text{ cm}$)
PF-1000 [8]-Poland	1064	12.2	2300	6.6	1.6×10^{10}	73.4
PF-360 [60]-Poland	130	6	1200	1.6	1.7×10^{10}	61.4
SPEED2 [11]-Chile	70	5.4	2400	2.7	1.2×10^{10}	270
7 kJ PF [63]-Japan	7	1.75	390	6	3.7×10^{10}	91
GN1 [13]-Argentina	4.7	1.9	—	—	1.9×10^{10}	—
Fuego Nuevo II [47]- Mexico	4.6	2.5	350	3.7	0.8×10^{10}	73
UNU/ICTP-PFF [4]- Asia and Africa	2.9	0.95	172	8.5	9.5×10^{10}	81
PACO [14, 47]- Argentina	2	2.5	250	1.5	3.6×10^9	95
PF-400J [31]-Chile	0.4	0.6	127	9	5.2×10^{10}	70
PF-50J [33]-Chile	0.07	0.3	60	9	7.3×10^{10}	66.7
	0.05	0.3	50	6	5.2×10^{10}	68

3. Discussion

3.1. Plasma energy density and drive parameter

A characteristic feature of the PF devices is that the plasma parameters remain relatively constant for facilities in a wide range of energy, from 1 kJ to 1 MJ, electron densities in the range $5 \times 10^{24} - 10^{26} \text{ m}^{-3}$, electron temperatures in the range 200 eV–2 keV and ion temperatures in the range 300 eV–1.5 keV. Another interesting feature is that the velocity of the current sheath is of the order of $1 \times 10^5 \text{ m s}^{-1}$ in the axial phase and of the order of $2.5 \times 10^5 \text{ m s}^{-1}$ in the pinch compression in every optimized PF, and in the optimized devices the plasma temperature is of the order of 1 keV. It is important to note that recently it has been demonstrated that it is possible to build plasma foci devices operating at hundreds and tens of joules (see section 2.1 and [31–33]). These compact devices reproduce the same plasma dynamics and pinch compression and emit x-rays and neutrons.

It is interesting to remark that plasma parameters practically constant in PF devices are correlated with the value of the electrical and geometrical parameters of the devices. This is useful for design considerations.

A comparison between plasma foci of different energies is necessary. Although only a fraction of the initial energy stored, E , in the capacitor bank is transferred to the plasma, the parameter E/V_p (with the plasma volume V_p) is usually used to characterize the plasma energy density in order to compare different devices. According to scaling laws [37] and optical diagnostics [30] the final pinch radius (previous to the appearance of instabilities with the subsequent appearance of smaller inhomogeneities in the plasma column) is of the order of $0.12a$, and the maximum pinch length is of the order of $0.8a$. Thus the final plasma volume, V_p (previous to the appearance of probable instabilities), is of the order of $\pi(0.12a^2) \times (0.8a) = 0.036a^3$, and the plasma energy density at the pinch moment is proportional to $E/V_p \sim 28E/a^3$. In table 3, the parameter $28E/a^3$ is listed for various

PF devices, and its value is of the order of $(1-10) \times 10^{10} \text{ J m}^{-3}$ [32]. The value of this energy density parameter in the case of the very small devices PF-400J and PF-50J is $(5-7) \times 10^{10} \text{ J m}^{-3}$.

Another relevant parameter in plasma foci is the drive parameter $(I_0/ap^{1/2})$ [37], where I_0 is the peak current, a is the anode radius and p is the gas filling pressure for the maximum neutron yield. This drive parameter $(I_0/ap^{1/2})$ is related to the velocity of the axial and radial phases of the plasma motion (of the order of $v_a = (0.8-1) \times 10^5$ and $v_r = (2-2.5) \times 10^5 \text{ m s}^{-1}$, respectively, for a wide range of PF sizes). In fact, the axial and radial velocities are proportional to $(I_0/ap^{1/2})$ [4, 35, 37]. For devices in the range of 3 kJ–1 MJ operating in deuterium, the drive parameter is $I_0/ap^{1/2} = 77 \pm 7 \text{ kA cm}^{-1} \text{ mbar}^{1/2}$ [20]. In table 3, the drive parameter $(I_0/ap^{1/2})$ is listed for various PF devices operating in deuterium, including the very small devices of 400 and 50 J. The drive parameter for the very small devices PF-400J and PF-50J is evaluated to be $\sim 70 \text{ kA cm}^{-1} \text{ mbar}^{1/2}$.

It is important to note that the parameters used in the design, construction and operation of the PF of SPEED2 give a drive parameter very high in comparison with the other devices listed in table 3. It is remarkable that if this parameter is experimentally increased over $95 \text{ kA cm}^{-1} \text{ mbar}^{1/2}$ (modifying I_0 , a or p) the PF does not work. This is the experience in most plasma foci [21]. However, in SPEED2 evidence of pinch has been observed, and the neutron yield has been measured with a high value of $(I_0/ap^{1/2})$. An exhaustive characterization of the neutron emission from the PF of SPEED2 is required to clarify this point.

3.2. Enhancement of the thermonuclear component of the neutron yield

As has been commented previously, the total neutron yield, Y , is $Y = Y_{\text{th}} + Y_{\text{b-t}}$, where Y_{th} is the thermonuclear component and $Y_{\text{b-t}}$ is the beam–target component. The possibility of enhancing the thermonuclear component of the neutron yield by increasing the drive parameter $(I_0/ap^{1/2})$ (i.e. the velocity of the current sheath) has been discussed by Serban and Lee [37]. They have proposed that as the square root of the pressure, $p^{1/2}$, varies very little (less than 40%) relative to the variation of I (ten times or more), (I/a) may be considered to have an almost fixed value for a wide range of devices. The pinch plasma in the range of 1 kJ to megajoules has practically the same temperature, $T \sim 1 \text{ keV}$, and density, $n \sim 10^{25} \text{ m}^{-3}$. The thermonuclear component of the neutron yield will thus be proportional to a^4 (a^3 from the volume dependence and another factor from the pinch lifetime dependence). This gives the well-known law $Y_{\text{th}} \propto I^4$ that is observed in PF devices. The above argument also suggests that this observed law is due to the fixed speed (or fixed energy density) operation over the whole range of PF machines. If the value of (I/a) is increased, the speed will increase with (I/a) , and T will increase with $(I/a)^2$. In the present range of operation of PF ($\sim 1 \text{ keV}$ when D_2 is used), increasing T will lead to an increase in a fusion cross section $\langle \sigma v \rangle$ proportional to T^ν , with $\nu \sim 4$, and thus $\langle \sigma v \rangle \sim (I/a)^8$. Thus $Y_{\text{th}} \sim \langle \sigma v \rangle$ (volume) (pinch lifetime) $\propto (I/a)^8 (a^3)(a) = (I/a)^4 I^4$. Thus, if (I/a) is a constant, this reduces to $Y_{\text{th}} \propto I^4$ as noted above. Otherwise $(I/a)^4 I^4$ (or $v^4 I^4$); if (a) is kept constant as I is increased, then $Y_{\text{th}} \propto I^8$. With this improved or enhanced yield dependent, the thermonuclear component of the neutron yield will rapidly outstrip the beam–target component. Assuming a simple inductive model for the beam acceleration in the beam target component of the neutron yield, the relation $Y_{\text{b-t}} \propto I^{9/2}/v^{3/2} \propto I^{9/2}/(I/a)^{3/2}$ was obtained in [44]. Thus in the limit, if a is kept constant while increasing I , $Y_{\text{b-t}} \propto I^3$ and $Y_{\text{th}} \propto I^8$. A composite anode was used (a one piece anode with the diameter reduced at the end) was used in [44] as a way of obtaining a PF operating with a high value of the drive parameter, and an enhancement of the order of 12–16% in the neutron yield was reported.

Further, the evidence of pinch and measured neutron yield obtained in the SPEED2 with a high value of $(I_0/ap^{1/2})$ deserves an extensive study and characterization of the neutron emission. On the other hand, from our experiments in plasma foci with hundreds and tens of joules (PF-400J and PF-50J in table 2) it is observed that the total neutron yield scaling is $Y \sim 7.73 \times 10^{-5} I_0^{4.82}$ (with I_0 in kA). This last observation motivates future experiments in order to determine the contribution of Y_{th} and Y_{b-t} to the total neutron yield and to corroborate this preliminary scaling law for the region of hundreds and tens of joules.

4. Scaling of a PF to energies lower than 1 J

Considering that the plasma energy density parameter $E/V_p = 28E/a^3$ and the drive parameter $(I_0/ap^{1/2})$ are practically constant in all PF devices operating in the range of 50 J to 1 MJ, we can question how low we can go in loading energy and still obtain the plasma and neutron emission.

Using the relation $28E/a^3 = 5 \times 10^{10} \text{ J m}^{-3}$, for a design of a PF of 0.25 J, for example, we immediately see that the anode radius must have a sub-millimetre size, $a \sim 0.5$ mm. A device with a capacity of 5 nF and an inductance of 5 nH, charged at 10 kV (0.25 J), produces a current peak $I_0 = 10$ kA in a short circuit. To produce a good ionization over the insulator, a pressure of $p = 3$ mbar should be used. Thus using the relation for deuterium $(I_0/ap^{1/2}) = 77 \text{ kA cm mbar}^{1/2}$ the anode radius is $a = 0.8$ mm. To determine the effective anode length, z_a , it is necessary to consider that the peak current must be coincident with the moment of the pinch, and so the relation $(z_a/v_a) + (a/v_r) = (T/4)$ is used ($v_a = 1 \times 10^5 \text{ m s}^{-1}$, the axial velocity, and $v_r = 2.5 \times 10^5 \text{ m s}^{-1}$, the radial velocity of the current sheath, are used, and T is the period of the discharge; in this case $T \sim 32$ ns). Thus the anode length is $z_a \sim 0.5$ mm. A device with these characteristics has been constructed at CCHEN [70, 71]. Details of the design and of the experimental observations are being published [71].

The current temporal derivative was measured using a Rogowski coil. The charging voltage was controlled using a resistive divider. Discharges in hydrogen at high pressure (20 mbar) were obtained to measure the electrical parameters of the device. Simultaneously, images from the plasma were obtained with a visible ICCD camera gated at 4 ns exposure time. It can be seen that the plasma remains attached to the insulator, which is consistent with the behaviour of PF discharges at high pressures. Essentially this discharge is a short-circuit, and therefore it can be used to calculate the electrical characteristics of the effective LC system, which work out to $C = 4.9$ nF, $T = 30$ ns, $L = 4.8$ nH. The first quarter of the period was 16 ns, which suggests that the time for creating the current sheath is of the order of 8 ns.

Figure 5 shows the electrical signals during a discharge in hydrogen at 3 mbar, with an initial charge of 6.5 kV (i.e. 0.1 J). A current peak of 4.5 kA was obtained. Figure 5 also shows a sequence of photographs of the evolving plasma. The following phenomena can be identified from the pictures: (a) the plasma is initiated over the insulator, (b) the plasma covers the anode, (c) there is a radial compression of the plasma over the anode and (d) the plasma separates from the anode in the axial direction. The time from stages (a) to (d) is about 30 ns.

Clear evidence that a radial compression (pinch) actually occurred is the dip observed in the current-derivative signal (the frequency change of the dI/dt oscillation; it was used as time zero in the graph), coinciding with a drop in the electrical current and a small peak in the voltage signal. In turn, the above-mentioned features were not observed in the electrical signals of the discharge at 20 mbar. Unfortunately, the temporal response of the voltage monitor is too slow to properly follow the fast changes in the discharge voltage; however, the frequency change of the dI/dt signal and the drop in the current are the evidence of the pinch.

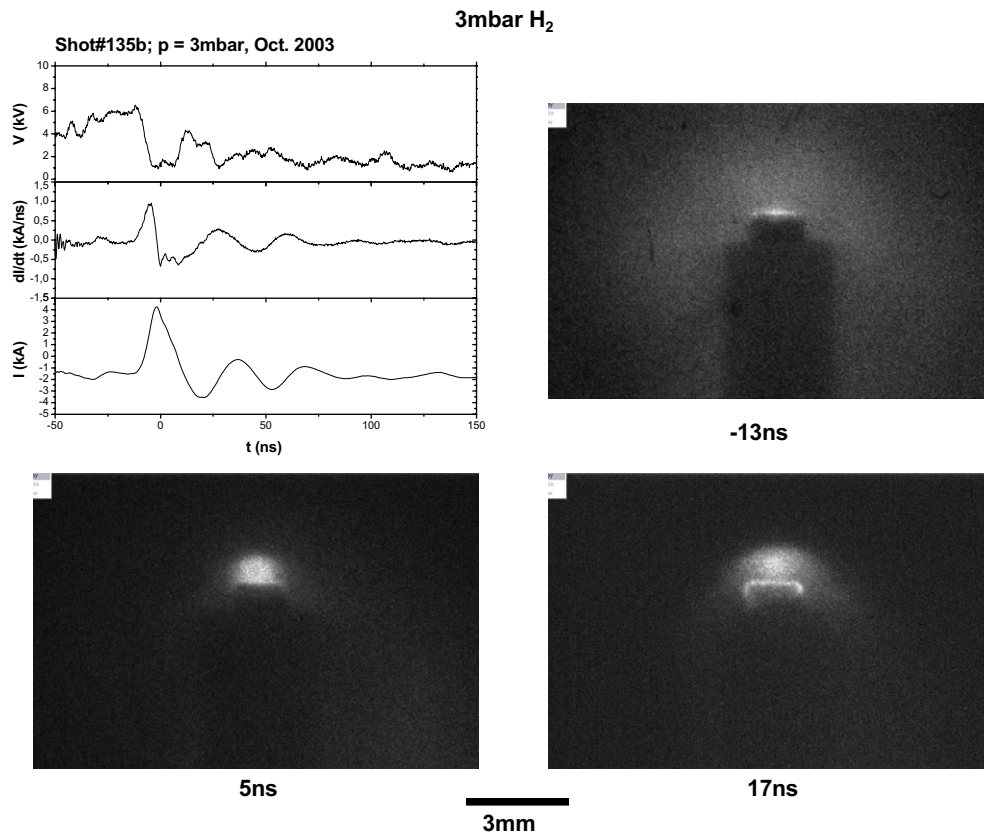


Figure 5. Electrical signals obtained in an ultra-miniature plasma focus operating in hydrogen at 3 mbar, with an initial charge of 6.5 kV (i.e. 0.1 J). A current peak of 4.5 kA was obtained. Clear evidence that a radial compression (pinch) actually occurred is the dip observed in the current-derivative signal (it is the frequency change of the dI/dt oscillation, and it was used as time zero in the graph), coinciding with a drop in the electrical current and a small peak in the voltage signal. The photographs correspond to a sequence of the evolving plasma. The following phenomena can be identified from the pictures: (a) the plasma is initiated over the insulator, (b) the plasma covers the anode, (c) there is a radial compression of the plasma over the anode and (d) the plasma separates from the anode in the axial direction. The time from stage (a) to (d) is about 30 ns.

The characteristic parameters of the miniaturized PF operating with hydrogen at 3 mbar were $E/V_p = 5.6 \times 10^9 \text{ J m}^{-3}$ and $I_0/(p^{1/2}a) = 33 \text{ kA mbar}^{-1/2} \text{ cm}$. To increase these parameters the current must be increased or the anode radius must be decreased. Both possibilities are currently in development. Measurements of neutrons and x-rays are also being implemented. In spite of considerations of optimization, it has been demonstrated that it is possible to scale a PF to operate with energies lower than 1 J [70, 71].

5. Final comments

An overview of the recent advances in the PF research has been presented in section 1 of this paper. Some topics were not considered in this paper, such as stability, micro instabilities, diagnostics, the role of the insulator covering the anode in the ionization process

and applications as a laboratory for astrophysical phenomena studies, among others. For these topics see [1, 8, 9, 20].

The most relevant results obtained at the CCHEN were presented in section 2 with emphasis on the development of miniaturized PF devices operating at very low energies (hundreds and tens of joules and less than 1 J, in section 4). This region of energy was unexplored until now. These results could serve to motivate a technological platform for engineering small portable repetitive plasma foci, thus getting a portable repetitive source of radiation ‘nanoflashes’.

The specific contribution of the thermonuclear fusion reactions and the ion beam–target fusion reactions to the total neutron yield emitted from pinch plasma foci are, as yet, an open field. One possibility of clarifying the contribution of the thermonuclear component versus the ion beam–target component to the total neutron yield could be by measuring the emission at several angles, as has been proposed by Castillo *et al* [47] and then trying to obtain empirical scale laws for both components of the neutron yield, the isotropic and anisotropic components. This approach is being implemented at CCHEN using several PF devices, ranging in energy from tens of joules to tens of kilojoules. In addition the possibility of enhancing the thermonuclear component of the neutron yield as has been proposed by Serban and Lee [37] is being studied at CCHEN. In addition, theoretical efforts must develop to obtain a model for the ion beam productions in pinches and a subsequent model applicable to the beam–target fusion in plasma foci. The collaboration with groups working in the experimental and theoretical study of neutron emission in other configurations could be useful. For example, in [86, 87] the neutron yield produced by ion beam–target fusion reactions has been computed and measured experimentally for a deuterated solid target irradiated by an ultra-intense laser pulse.

Several applications have been commented on in this paper, and the next step should be to design optimized PF devices for specific applications outside the laboratory, for example, radiographies. Several engineering subjects must be considered and solved. The detection of substances using plasma foci is still an open field and is waiting to be seriously considered. The same applies to the possible production of radioisotopes for nuclear medicine. Other industrial applications have been proposed by Gribkov in [82]. The potential applications of this kind of intense pulse of radiation emitted by pinch discharges motivates the study of their effects in cells, and interdisciplinary work with biologists is required. Some efforts in this area have been made in Russia [72].

An integrated discussion placing more emphasis on the common features of the PF experiments and devices rather than on their differences was presented in section 3. The plasma density and drive parameter were discussed. The fact that the plasma energy parameter and the drive parameter are practically constant for all the plasma foci operating in a wide range of energies, from tens of joules to megajoules, constitutes a useful tool of design. However, these observations must be theoretically explained.

Using the drive parameter like a design tool, a PF operating at only 0.1 J has been designed and constructed (section 4). At what energy are these scaling rules not valid? When do the plasma surface effects start to be relevant? Could these effects be favourable for increasing the plasma energy density for much smaller devices, improving the generation of fusion reactions and radiation?

Acknowledgments

The author appreciates the collaboration of P Silva, J Moreno, M Zambra, G Sylvester, C Pavez and A Tarifeño from the Plasma Physics and Plasma Technology Group at CCHEN (Chile) and the comments and suggestions of H Bruzzone, A Clause, M Barbaglia, M M Milanese

(Argentina), F Castillo and J Herrera (Mexico), S Lee (AAAPT), M Zakaullah (Pakistan), K Tomaszewski (Poland) and B Stewart (ICTP). Work has been supported by FONDECYT grant 1030062 (Chile).

References

- [1] Bernard A *et al* 1998 *J. Moscow Phys. Soc.* **8** 93
- [2] Filipov N V, Filipova T I and Vinogradov V P 1962 *Nucl. Fusion* **2** (Suppl.) 577
- [3] Mather J W 1964 *Phys. Fluids* **7** (Suppl.) 28
- [4] Lee S *et al* 1988 *Am. J. Phys.* **56** 62
- [5] Zakaullah M, Alamgir K, Shafiq M, Hassan S M, Sharif M, Hussain S and Waheed A 2002 *Plasma Sources Sci. Technol.* **11** 377
- [6] Szydłowski A, Scholz M, Karpinski L, Sadowski M, Tomaszewski K and Paduch M 2001 *Nukleonika* **46** (Suppl. 1) S61
- [7] Tafreshi M A *et al* 2001 *Nukleonika* **46** (Suppl. 1) S85
- [8] Schdmidt H, Kasperczuk A, Paduch M, Pisarczyk T, Scholz M, Tomaszewski K and Szydłowski A 2002 *Phys. Scr.* **66** 168
- [9] Scholz M, Bienkowska B, Ivanova-Stanik I, Karpinski L, Miklaszewski R, Paduch M, Stepniewski W and Tomaszewski K 2004 *Czech. J. Phys.* **54** (Suppl. C) C170
- [10] Czekaj S, Kasperczuk A, Miklaszewski R, Paduch M, Pisarczyk T and Wereszczynski Z 1989 *Plasma Phys. Control. Fusion* **31** 587
- [11] Decker G, Kies W, Mälzig M, Van Valker C and Ziethen G 1986 *Nucl. Instrum. Methods A* **249** 477
- [12] Soto L *et al* 2004 *Braz. J. Phys.* **B 34** 1814
- [13] Moreno C, Bruzzone H, Martinez J and Clausse A 2000 *IEEE Trans. Plasma Sci.* **28** 1735
- [14] Pouzo J and Milanese M 2003 *IEEE Trans. Plasma Sci.* **31** 1237
- [15] Silva P and Favre M 2002 *J. Phys. D: Appl. Phys.* **35** 2543
- [16] Castillo F *et al* 2002 *Braz. J. Phys.* **32** 3
- [17] Guo Zh G, Han M, Pu Y K and Wang X X 2002 *Book of Abstracts: 14th Int. Conf. on High-Power Particle Beams and 5th Int. Conf. on Dense Z-pinchs (Albuquerque, USA, 2002)* p 77
- [18] Beg F N, Krushelnick K, Gower C, Torn S and Dangor A E 2002 *Appl. Phys. Lett.* **80** 3009
- [19] Gupta R and Srivastava M P 2004 *Plasma Sources Sci. Technol.* **13** 371
- [20] Rawat R S, Zhang T, Phua C B L, Then J X Y, Chandra K A, Lin X, Patran A and Lee P 2004 *Plasma Sources Sci. Technol.* **13** 569
- [21] Gibbons M, Richards W and Shields K 1998 Optimization of neutron tomography for rapid H concentration inspection of metal castings *LLNL Report UCRL-JC-129723*
- [22] Hussein E and Waller E 1998 *Radiat. Meas.* **29** 581
- [23] Lee S, Kudryashov V, Lee P, Zhang G, Serban A, Liu M, Feng X, Springham S, Wong T and Selvam C 1998 *ICPP and 25th EPS Conf. on Controlled Fusion and Plasma Physics* vol 22C, p 2591
- [24] Lebert R, Engel A, Bergmann K, Treichel O, Gavrilescu C and Neff W 1997 *4th Int. Conf. on Dense Z-pinchs (Vancouver, Canada) (New York: AIP) AIP Conf. Proc.* **409** 291
- [25] Prasad G, Krishnan R, Mangano M, Greene J and Niansheng P Oi 1993 *20th IEEE Int. Conf. on Plasma Science (Vancouver, Canada, 1993)* p 185
- [26] Lee S, Lee P, Zhang G, Feng X, Gribkov V, Liu M, Serban A and Wong T 1998 *IEEE Trans. Plasma Sci.* **26** 1119
- [27] Rapezzi L, Angelone M, Pillon M, Rapisarda M, Rossi E, Samuelli M and Mezzetti F 2004 *Plasma Sources Sci. Technol.* **13** 272
- [28] Soto L, Esaulov A, Moreno J, Silva P, Sylvester G, Zambra M, Nazarenko A and Clausse A 2001 *Phys. Plasmas* **8** 2572
- [29] Silva P, Soto L, Moreno J, Sylvester G, Zambra M, Altamirano L, Bruzzone H, Clausse A and Moreno C 2002 *Rev. Sci. Instrum.* **73** 2583
- [30] Moreno J, Silva P and Soto L 2003 *Plasma Sources Sci. Technol.* **12** 39
- [31] Silva P, Moreno J, Soto L, Birstein L, Mayer R and Kies W 2003 *Appl. Phys. Lett.* **83** 3269
- [32] Silva P, Soto L, Kies W and Moreno J 2004 *Plasma Sources Sci. Technol.* **13** 329
- [33] Soto L, Silva P, Moreno J, Zambra M, Kies W, Mayer R E, Bruzzone H, Altamirano L, Huerta L and Clausse A Demonstration of neutron production from a deuterium plasma pinch driven by a capacitor bank charged at only tens of joules, submitted
- [34] Moreno C, Bruzzone H, Martinez J and Clausse A 2000 *IEEE Trans. Plasma Sci.* **28** 1735

- [35] Lee S 1985 *Laser and Plasma Technology* ed S Lee *et al* (Singapore: World Scientific).
- [36] Kromholz H, Ruhl F, Schneider W, Schonbach K and Herziger G 1981 *Phys. Lett. A* **82** 82
- [37] Lee S and Serban A 1996 *IEEE Trans. Plasma Sci.* **24** 1101
- [38] Milanese M and Pouzo J 1985 *Nucl. Fusion* **25** 840
- [39] Pouzo J, Cortázar D, Milanese M, Moroso R and Piriz R 1988 *Small Plasma Physics Experiments (Singapore: World Scientific)* p 80
- [40] Milanese M and Pouzo J 1988 *Small Plasma Physics Experiments* (Singapore: World Scientific) p 66
- [41] Pouzo J 1997 *Proc. Int. Symp. on Plasma Research and Application: PLASMA'97 (Polonia, 1997)* vol 2, p 65
- [42] González P, Florido P, Bruzzone H and Clause A 2004 *IEEE Trans. Plasma Sci.* **32** 1383
- [43] Moreno C, Casanova C, Correa C and Clause A 2003 *Plasma Phys. Control. Fusion* **45** 1989
- [44] Serban A and Lee S 1998 *J. Plasma Phys.* **60** 3
- [45] Moo S P, Chakrabarty C K and Lee S 1991 *IEEE Trans. Plasma Sci.* **19** 515
- [46] Aliaga-Rossel R and Choi P 1998 *IEEE Trans. Plasma Sci.* **26** 1138
- [47] Castillo F, Herrera J J E, Rangel J, Milanese M, Moroso R, Pouzo J, Golarri J I and Espinosa G 2003 *Plasma Phys. Control. Fusion* **45** 289
- [48] Zakaullah M, Alamgir K, Shafiq M, Hassan S M, Sharif M and Waheed A 2001 *Appl. Phys. Lett.* **78** 877
- [49] Hussain S, Ahmad S, Khan M Z, Zakaullah M and Waheed A 2003 *J. Fusion Energy* **22** 195
- [50] Venere M, Moreno C, Clause A, Barbuza R and Del Fresno M 2001 *Nukleonika* **46** (Suppl. 1) S93
- [51] Moreno C, Clause A, Martínez J F, Llovera R and Tartaglione A 2001 *Nukleonika* **46** (Suppl. 1) S33
- [52] Clause A 2004 private communication
- [53] Nayak B B, Acharya B S, Mohanty S R, Borthakur T K and Bhuyan H 2001 *Surf. Coat. Technol.* **145** 8
- [54] Bhuyan H, Mohanty S R and Borthakur T K 2001 *Indian J. Pure Appl. Phys.* **39** 698
- [55] Mohanty S R, Bhuyan H, Neog K K, Nayak B B, Acharya B S and Rout R K 2002 *Power Mater. Process.* 681
- [56] Zakaullah M, Waheed A, Ahmad S, Shaista Zeb and Hussain S 2003 *Plasma Sources Sci. Technol.* **12** 443
- [57] Kies W, Decker G, Bemtien U, Sidelnikov Yu V, Glushkov D A, Koshelev K N, Simanovskii D M and Bobashev S V 1999 *Tech. Phys. Lett.* **25** 802
- [58] Kubes P *et al* 2002 Dense Z-pinches *5th Int. Conf. on Dense Z-pinch (Albuquerque, USA, 2001)* *AIP Conf. Proc.* **651** 193
- [59] Stanislavski J, Baranowski J, Sadowski M and Zebrowski J 2001 *Nukleonika* **46** (Suppl. 1) S73
- [60] Zebrowski J, Baranowski J, Jakubowski L and Sadowski M 2001 *Nukleonika* **46** (Suppl. 1) S65
- [61] Baranowski J, Jakubowski L, Sadowski M and Zebrowski J 2001 *Nukleonika* **46** (Suppl. 1) S69
- [62] Etaati G R, Abbasi Davani F, Babazadeh A R and Yousefi H R 2004 *12th Int. Congr. on Plasma Physics: Book of Abstracts (Nice, Francia, 2004)* p 215
- [63] Kashani M A M and Miyamoto T 2002 Dense Z-pinches *5th Int. Conf. on Dense Z-pinch (Albuquerque, USA, 2001)* *AIP Conf. Proc.* **651** 249
- [64] Soto L, Chuaqui H, Favre M and Wyndham E 1994 *Phys. Rev. Lett.* **72** 2891
- [65] Soto L, Chuaqui H, Favre M, Saavedra R, Wyndham E, Skowronek M, Romeas P, Aliaga-Rossel R and Mitchell I 1998 *IEEE Trans. Plasma Sci.* **26** 1179
- [66] Esaulov A, Sasorov P, Soto L and Zambra M 2001 *Phys. Plasmas* **8** 1395
- [67] Soto L and Clause A 2003 *Phys. Scr.* **67** 77
- [68] Kies W private communication
- [69] Moreno J, Birstein L, Mayer R E, Silva P and Soto L Measurement of low yield neutron pulses from D–D fusion reactions using a ^3He proportional counter, submitted
- [70] Soto L, Pavez C, Barbaglia M, Clause A and Moreno J 2004 *12th Int. Congr. on Plasma Physics: Book of Abstracts (Nice, Francia, 2004)* p 218
- [71] Soto L, Pavez C, Barbaglia M, Clause A and Moreno J Scaling of a plasma focus to energies lower than 1 J, submitted
- [72] Dubrosky V, Gazaryan I G, Gribkov V A, Ivanov Yu P, Kost O A, Orlova M A and Troshina N N 2003 *J. Russ. Laser Res.* **24** 289
- [73] Raspa V, Silva P, Moreno J, Zambra M and Soto L 2004 *12th Int. Congr. on Plasma Physics: Book of Abstracts (Nice, Francia, 2004)* p 103
- [74] Lerner E J 2003 Towards advanced-fuel fusion: electron, ion energy > 100 keV in a dense plasma *Conf. Current Trends in International Fusion Research (Washington, USA, 2003)*
- [75] Haines M G, LePell P D, Coverdale C A and Deeney C 2004 *12th Int. Congr. on Plasma Physics: Book of Abstracts (Nice, Francia, 2004)* p 92
- [76] Potter D E 1971 *Phys. Fluids* **21** 1911
- [77] Czaus K, Sadowski M J and Zebrowski J 2001 *CD Proc. Int. Symp. Plasma 2001 (Warsaw, Poland, 2001)* p 3.5

- [78] Jakubowski L, Sadowski M, Baranova E O and Vikherev V V 1997 *4th Int. Conf. on Dense Z-pinches (Vancouver, Canada) AIP Conf. Proc.* **409** 443
- [79] Baranova E O, Sholin G V and Jakubowski L 2003 *Plasma Phys. Control. Fusion* **45** 1071
- [80] Jakubowski L, Sadowski M and Zebrowski J 2001 *Nucl. Fusion* **41** 755
- [81] Rafique M S, Springham S V, Patran A and Lee S 2000 *Proc. 10th Int. Congr. on Plasma Physics* vol 2 (*Quebec, Canada, 2000*) p 520
- [82] Gribkov V A 2001 *CD Proc. Int. Symp. Plasma 2001 (Warsaw, Poland, 2001)* I9.1
- [83] Heo H and Park D K 2002 *Phys. Scr.* **65** 350
- [84] Pasternak A and Sadowski M 2001 *Nukleonika* **46** (Suppl. 1) S29
- [85] Gribkov V A *et al* 2003 *J. Phys. D: Appl. Phys.* **36** 1817
- [86] Disdier L, Garçonnet J P, Malka G and Miquel J L 1999 *Phys. Rev. Lett.* **82** 1454
- [87] Toupin C, Lefebvre E and Bonnaud G 2001 *Phys. Plasmas* **8** 1011